Available online at www.sciencedirect.com

ScienceDirect

Procedia IUTAM 25 (2017) 74–81

Procedia IUTAM

www.elsevier.com/locate/procedia

IUTAM Symposium on Storm Surge Modelling and Forecasting

Estimation of extreme hydrodynamic environments of Puti Island wind farm in Bohai Sea

Jifu Zhou[a,b,*], Jinlong Liu[c]

[a]*Key Laboratory for Mechanics in Fluid Solid Coupling Systems, Institute of Mechanics, Chinese Academy of Sciences, Beijing 100190, China*

[b]*School of Engineering Sciences, University of Chinese Academy of Sciences, Beijing 100049, China*

[c]*China National Offshore Oil Corp Research Institute, Beijing 100028, China*

Abstract

In order to manifest the extreme hydrodynamic environments for Puti Island wind farm in Bohai Sea, flow and wave climates in the area induced by cold waves are investigated. According to the historical meteorology statistics and taking the global climate change into account, three typical paths (NNE, ENE and NNW) with four high wind speeds for cold waves in Bohai Sea are presumed. After calibrated with field data, the Princeton Ocean Model (POM) and the third-generation wave model, SWAN, are employed to delineate possible extreme hydrodynamic conditions in the area of Puti Island wind farm. The dependence of the extreme current and water wave parameters to the wind speed and wind direction is investigated. The distribution of the extreme current and water wave parameters in the wind farm is discussed.

Selection and peer-review under responsibility of IUTAM Symposium on Storm Surge Modelling and Forecasting.

Keywords: wind farm; Bohai; hydrodynamic environment

1. Introduction

An offshore wind farm is under construction nearby Puti Island, Bohai Sea, China (see Fig.1). It is called Puti Island wind farm. The water depth of the wind farm varies from 7*m* to 27*m*. For offshore wind turbines, a highly reliable foundation is of the most significance for the long-term operation of the turbines. However, since it works in

* Corresponding author. Tel.: +86-010-82544203.
E-mail address: zhoujf@imech.ac.cn

2210-9838
Selection and peer-review under responsibility of IUTAM Symposium on Storm Surge Modelling and Forecasting.
10.1016/j.piutam.2017.09.012

unsheltered conditions all the time, the foundation is vulnerable to harsh marine environments, which should be made clear prior to the construction of the project.

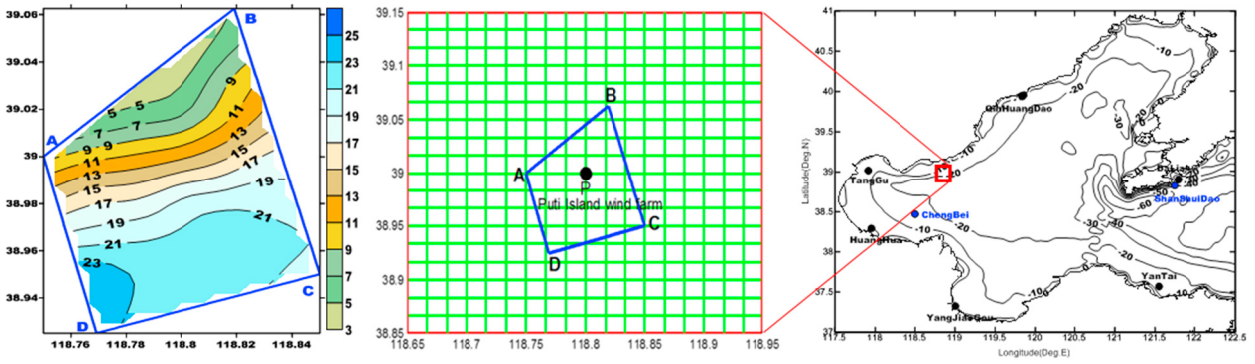

Fig. 1 The topography of Bohai Sea with the tide gauge stations in it and the location of the Puti Island wind farm bounded by the quadrilateral ABCD. The two blue tide stations collect data of current velocity and direction. The middle figure shows the refined nested area for computing hydrodynamics of Puti Island wind farm. The left figure shows the contour of water depth below still water level in Puti Island wind farm.

Bohai Sea, China, located in the mid-latitudes, is an area frequently hit by cold waves in autumn and winter. It is statistically shown from the meteorological data from 1991 to 2000 that 90.53 percent of wind speed over 12 *m/s* is caused by cold waves in Bohai Sea[1]. For Puti Island wind farm, potential damage and failure to the turbine foundation may occur due to the intense hydrodynamic forces exerted by the extreme currents and waves caused by cold waves. Therefore, current flow and wave climates in case of extreme cold waves are of crucial concern to the engineers.

In the present paper, we aim to manifest the extreme hydrodynamic environments for Puti Island wind farm in Bohai Sea. The flow and wave climates in the area induced by cold waves are investigated by means of the Princeton Ocean Model (POM) and the third-generation wave model, SWAN, respectively. According to the historical meteorology statistics and taking the global climate change into account, three typical paths (NNE, ENE and NNW) with four high wind speeds for cold waves in Bohai Sea are presumed. After calibrated with field data, the two models are employed to delineate possible extreme hydrodynamic conditions in the area of Puti Island wind farm. The relationships between the extreme hydrodynamic conditions and the cold wave path and wind speed are analyzed.

2. Model Configuration and Validation

2.1. Configuration and validation of POM

In order to validate POM in Bohai Sea, two simulations were performed respectively: one for the astronomical tide in Feb, 1988 and the other for the cold wave in Oct, 2003. The simulated domain for model validation is 117.5°E~122.5°E, 37°N~41°N (Fig. 1), which covers the whole Bohai Sea. Both meridian and zonal grid spacing are taken as 1', corresponding to the distance between two adjacent grid points being 1400*m* and 1850*m* in latitude and longitude, respectively. The whole water depth is divided into 12 layers. Initial water level and flow velocity are set to zero by using the cold start mode. At the open boundaries, the water elevations from TPXO assimilation model, version 7.2 (available at http://volkov.oce.orst.edu/tides/global.html), are used. The time-dependent water elevations consist of eight main astronomical tide components, which is highly accurate enough in coastal and shallow waters. The bottom topography is obtained from Global Topography, version 17.1 (available at http://topex.ucsd.edu/marine_topo/mar_topo.html).

In POM, the bottom friction coefficient C_z is determined by the logarithmic law and given by

$$C_z = MAX\left[\frac{\kappa^2}{\left[\ln\left\{(1+\sigma_{kb-1})H / z_0\right\}\right]^2}, 0.0025\right] \tag{1}$$

where κ=0.4 is the von Karman constant, H is the bottom topography, z_0 is the roughness parameter and σ_{kb-1} is the σ coordinate at the first grid near the bottom. If $(1+\sigma_{kb-1})H / z_0$ is large enough, C_z reverts to a constant value 0.0025. By comprehensive trials we have found that equation (1) is not a suitable way to parameterize C_z in Bohai Sea. As a matter of fact, taking the friction coefficient as a constant has been widely used[2,3,4]. Further numerical experiments demonstrate that setting the friction coefficient as 0.001 in the whole Bohai Sea is rather a proper choice to hind cast the astronomical tide in Feb, 1988 and the cold wave in Oct, 2003.

Comparison between the computed and the measured results are shown in Fig .2. It is shown that the simulated tides agree well with the observations, except the discrepancies at Tanggu and Qinhuangdao stations during the early period, which is owing to the cold start of the simulation and long distance of these two stations from the open boundary of Bohai Sea.

The simulated flow velocity is consistent with the measurement (Fig. 3), with the maximum difference not exceed 0.2*m/s*. The flow direction is also well reproduced. The only exception is that at Shanshuidao station around the 60th hour. This is because the flow velocity at Shanshuidao station around the 60th hour is very small. A slight error of velocity components can make a large change in the flow direction.

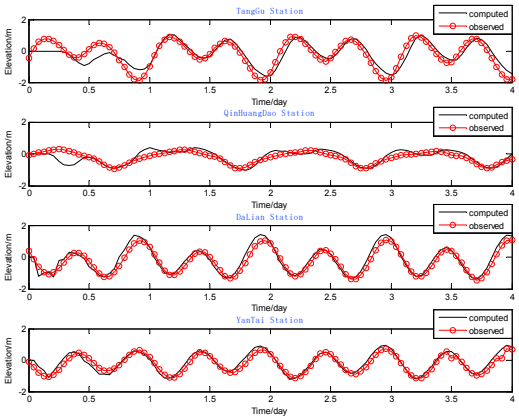

Fig. 2 Time series of computed and observed sea level at Tanggu, Qinhuandao, Dalian and Yantai gauge stations.

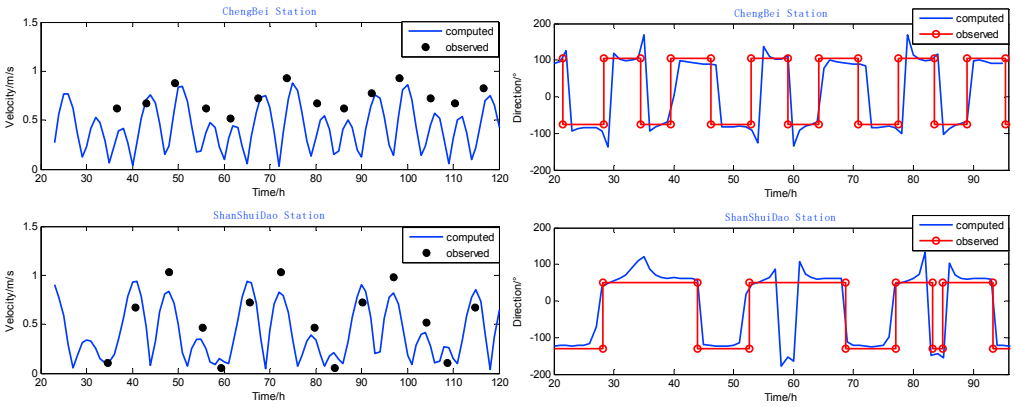

Fig. 3 Comparison between computed and observed current velocity and its direction at Chengbei and Shanshuidao stations.

Furthermore, a simulation of current flow induced by the cold wave occurring in October 2003 is also performed to show the ability of POM. The cold wave is very extreme due to the concurrence of spring tide. To simulate this cold wave, we selected the QSCAT/NCEP blended wind products with a spatial resolution of 0.5 degrees and a temporal resolution of six hours. The simulation time was from Oct. 9 to Oct. 13, 2003. Fig.4 presents the comparison of computed and measured surges during the cold wave at Yangjiaogou and Huanghua stations, which shows a satisfactory agreement between them, both in surge amplitude and phase. However, there are some differences between the measured data and the numerical results in the period of 50 ~ 60 hours at Huanghua, and in the period of 60 ~ 70 hours at Yangjiaogou. Nonetheless, due to the low accuracy of the wind field in both time and space, we deem that POM is capable of further investigating cold-wave-induced flow field in Bohai Sea.

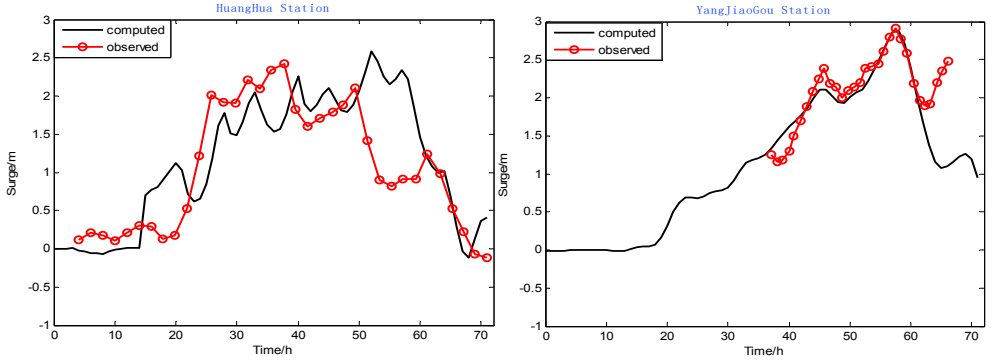

Fig. 4. The comparison of computed and measured cold surges in Yangjiaogou and Huanghua.

2.2. Configuration and validation of SWAN

A simulation of wind wave process in April, 2007 is performed to calibrate SWAN in Bohai Sea. The computation domain is 117.5°E~122.5°E, 37°N~41°N and the horizontal grid spacing is 2 minutes. In the computation, the QSCAT/NCEP blended wind field is also used. The expressions of wind input and white capping dissipation from Komen are adopted. The measured point is located at (118.8924° E, 38.3013° N) with a measured period from Apr. 11, 2007 to Apr. 17, 2007. The initial condition is by default a JONSWAP spectrum. To eliminate the effect of the initial condition, we start the simulation from April 9. Fig. 5 presents the comparison between computed and measured significant wave height and wave period. Although there are some differences between the two, the SWAN model reproduces the main feature of the wave field of Bohai Sea.

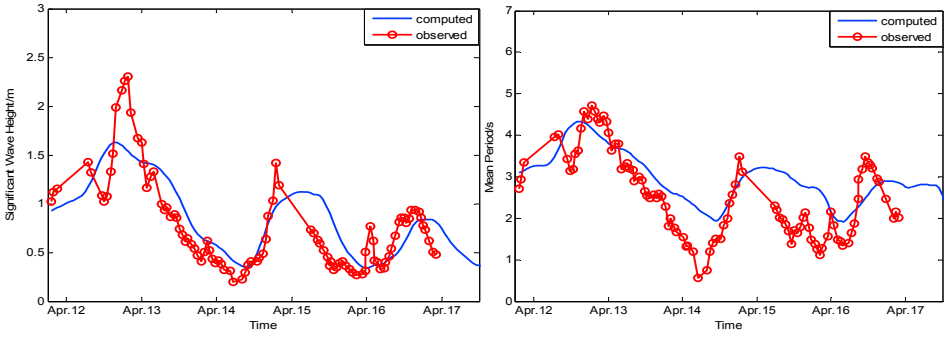

Fig. 5. The comparison of computed and measured significant wave height and mean wave period.

3. Results and Discussion

By means of POM and SWAN, we have investigated the hydrodynamic climates of Puti Island wind farm in case of typical extreme cold waves in Bohai Sea. In the wind farm area, a nested computational grid with horizontal resolution of 0.25' is used to improve the numerical accuracy without significant computational cost. The nested area is 118.65°E~118.95°E, 38.85°N~39.15°N (see Fig. 1). The boundary conditions are from the coarser grid results.

3.1. Typical extreme cold waves in Bohai Sea

Since Bohai Sea is very shallow with an average water depth of 18 *m*, the impact of atmospheric pressure on water flow is far less important than wind shear. Hence, we primarily consider the wind field of cold waves. In the present paper we focus on the extreme conditions. The wind speed considered is no less than 20.7 *m/s*. The horizontal spatial scale of cold waves is generally much larger than the dimension of Bohai Sea. So, the wind field can be viewed as spatially uniform. In regard to the wind direction, after analyzing the meteorological data from 1991 to 2000, Zhang (2003) revealed that cold waves hitting Bohai Sea move along three major tracks (NW, N, W), with each track having its own prevailing wind. As a result, we choose three typical cold wave paths (NW, N, W) for the numerical simulation which will induce NNE, ENE and NNW prevailing winds respectively. And for each path four wind speeds (20.7 *m/s*, 24.4 *m/s*, 28.7 *m/s* and 30*m/s*) are considered, the first three corresponding to winds of force 8 to 10, and the last one accounting for possible increase in extreme wind speed in the context of global climate change[5].The duration of cold air break is about a day or so. We take the extreme case of two days. Tab. 1 lists the presumed 12 cases.

Table 1. Presumed typical extreme cold waves hitting Bohai Sea.

Cold wave path	Prevailing wind	Wind speed (*m/s*)			
NW	NNE	20.7	24.4	28.7	30
N	ENE	20.7	24.4	28.7	30
W	NNW	20.7	24.4	28.7	30

3.2. Extreme water level and currents in Puti Island wind farm

In Bohai Sea, the NNE and ENE winds generally cause water level rise, while the NNW wind, which is offshore, makes water level decline. Both of the highest and lowest water levels during the operation of offshore structures are of significant concern. Here, we present the extreme high water level in case of the NNE and ENE winds, and the lowest water level in case of the NNW wind.

As seen in Tab. 2, the highest water level occurs in case of ENE wind. Fig. 6 shows the contours of water level in the wind farm for different wind directions with wind speed of 30*m/s*, suggesting a roughly uniform distribution of the highest water level, with the difference between the maximal and minimal values no more than 0.2 *m* for each case.

Table 2. Extreme water level in case of typical extreme cold waves.

Wind speed (*m/s*)	30	28.4	24.4	20.7
Highest water level in case of NNE wind (*m*)	2.29	1.99	1.59	1.22
Highest water level in case of ENE wind (*m*)	3.98	3.54	2.58	1.85
Lowest water level in case of NNW wind (*m*)	-2.32	-2.02	-1.54	-1.18

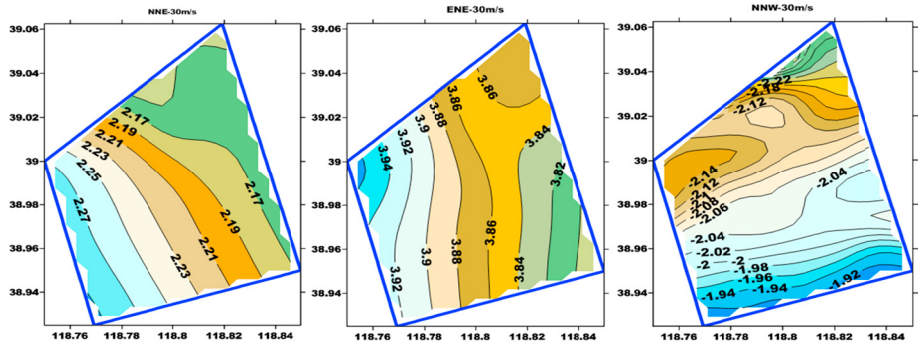

Fig. 6 Contours of water level in the wind farm for three wind directions with wind speed of 30*m/s*.

In Tab. 3, we present the maximum current velocity in case of the 12 cold waves. Unlike the highest water level which occurs in case of ENE wind, the maximum current velocity occurs in case of NNE wind. Fig. 7 shows the contours of maximum current velocity in the wind farm induced by NNE, ENE and NNW winds with wind speed of 30*m/s*, suggesting a roughly inverse dependence of the maximum current velocity to the water depth, i.e. larger current velocity occurring in the shallower area.

Table 3. Extreme current velocity in case of typical extreme cold waves.

Wind speed (*m/s*)	30	28.4	24.4	20.7
Maximum velocity in case of NNE wind (*m/s*)	3.82	3.73	3.63	2.94
Maximum velocity in case of ENE wind (*m/s*)	3.50	3.19	2.61	2.26
Maximum velocity in case of NNW wind (*m/s*)	1.92	1.88	2.2	2.19

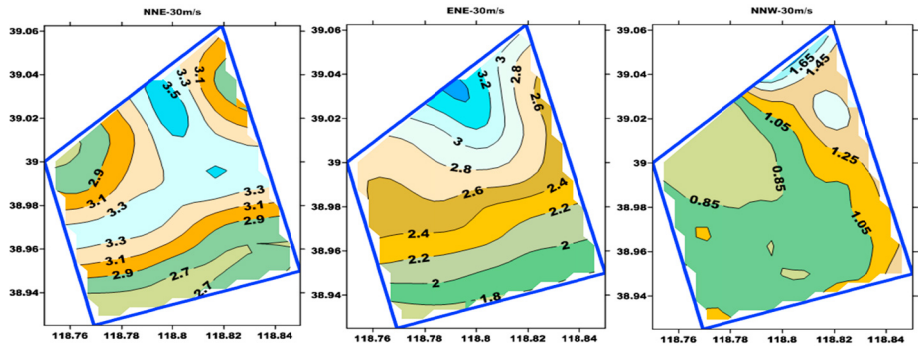

Fig. 7 Contours of maximum current velocity in the wind farm for three wind directions with wind speed of 30*m/s*.

3.3. Extreme waves in Puti Island wind farm

Extreme wave parameters, such as the significant wave height and the wave period, are of crucial significance for estimating wave force to marine structures. Here, we extract the extreme values of these two parameters from the simulated data.

In Tab. 4, we list the highest significant wave height in the wind farm area for different wind directions with different wind speeds. Higher wind speeds cause higher waves. The ENE wind makes higher wave than the NNE and NNW winds. Fig. 8 displays contours of the significant wave height in the wind farm for ENE, NNE and NNW winds with wind speed of 30*m/s*. It can be seen that the contours are generally parallel to the contours of the bottom

topography (see Fig. 1), suggesting that water depth takes an important role in the wave height estimation. Higher waves occur in deeper water area.

Table 4. Extreme significant wave height in case of typical extreme cold waves.

Wind speed (*m/s*)	30	28.4	24.4	20.7
Maximum significant wave height in case of ENE wind (*m*)	6.87	6.76	6.28	5.41
Maximum significant wave height in case of NNE wind (*m*)	5.97	5.77	5.10	4.24
Maximum significant wave height in case of NNW wind (*m*)	4.49	4.24	3.64	3.05

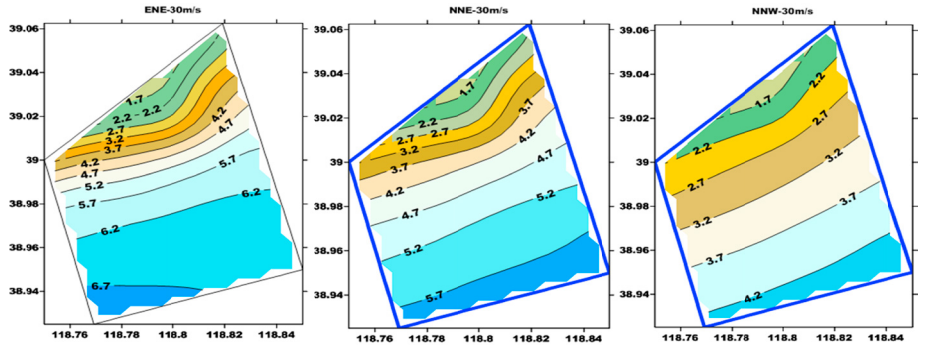

Fig. 8 Contours of significant wave height in the wind farm for three wind directions with wind speed of 30*m/s*.

In Tab. 5, we list the maximum wave period in the wind farm area with different wind cases. Although higher wind speeds cause longer wave periods, the wind speed does not make much difference to the maximum wave period. Wind directions have more effect on the maximum wave period. The ENE wind makes longer wave period than the NNE and NNW winds. Fig. 9 displays contours of the average wave period in the wind farm for ENE, NNE and NNW winds with wind speed of 30*m/s*. It also shows that the contours are generally parallel to the contours of the topography (see Fig. 1), suggesting that water depth takes an important role in average wave period estimation. In deeper water area, the average wave period is longer.

Table 5. Maximum wave period in case of typical extreme cold waves.

Wind speed (*m/s*)	30	28.4	24.4	20.7
Maximum wave period in case of NNE wind (*s*)	6.61	6.55	6.31	5.93
Maximum wave period in case of ENE wind (*s*)	7.47	7.45	7.37	7.14
Maximum wave period in case of NNW wind (*s*)	5.42	5.33	5.06	4.74

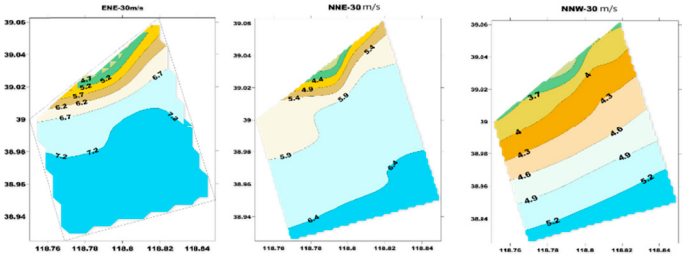

Fig. 9 Contours of the average wave period in the wind farm for three wind directions with wind speed of 30 *m/s*.

4. Conclusion

Using field data, we have calibrated the POM and SWAN models in Bohai Sea. Then, we have employed the two models to delineate possible extreme hydrodynamic conditions in the area of Puti Island wind farm in Bohai Sea. Conclusions are drawn as follows.

Extreme hydrodynamic conditions in the area of Puti Island wind farm occurs in case of cold waves. Both the wind direction and the wind speed during cold waves are influential parameters to the extreme water currents and waves.

At the same wind speed, the highest water level and the maximum current velocity occur in different wind directions. The ENE wind makes the highest water level, whereas the NNE wind makes the maximum current velocity. The highest water level roughly displays a uniform distribution in the wind farm. The maximum current velocity is roughly inverse proportional to the water depth.

Wind direction is more influential to water wave parameters than wind speed. At the same wind speed, the ENE wind makes higher waves with longer periods than the NNE and NNW winds. The contours of the significant wave height and the average wave period are generally parallel to the contours of bottom topography, suggesting that water depth is an important parameter governing the extreme wave parameters. Higher waves with longer periods occur in deeper water areas.

Acknowledgements

We would like to give thanks to the financial support from the National Natural Science Foundation of China (Grant Nos. 11232012, 11172307 and 11572332), the National 973 Program (Grant No. 2014CB046200) and the Strategic Priority Research Program of the Chinese Academy of Sciences (Grant XDB22040203).

References

1. Zhang XH. The statistical characteristics and physical mechanism of strong wind in Bohai Sea. Ocean University of China; 2003. (in Chinese)
2. Zhao BR, Fang GH, Cao DM. Numerical simulation of tide and tidal Current in the Bohai, Yellow and East China Seas. *ACTA OCEANOLOGICA SINICA*1994;**5**:1-10. (in Chinese)
3. Wan ZW, Qiao FL, Yuan YL. Three-dimensional numerical modelling of tidal waves in the Bohai, Yellow and East China Seas. *OCEANOLOGIA ET LIMNOLOGIA SINICA*1998;**6**:611-616. (in Chinese)
4. Lee JC, Jung KT. Application of eddy viscosity closure models for the M2 tide and tidal currents in the Yellow Sea and the East China Sea. *Cont Shelf Res* 1999; **19(4)**: 445-475.
5. Wang LZ, Li JC. Estimation of extreme wind speed in SCS and NWP by anon-stationary model. *Theoretical and Applied Mechanics Letters* 2016; **6**:131-138.